

Article

Development of Advanced Pea Breeding Lines with Improved Resistance to Ascochyta Blight

Manuel Alejandro Jiménez-Vaquero ^{1,2,*} , María José Cobos ¹ , Carmen María Ruiz-Pastor ¹ and Diego Rubiales ¹ 

¹ Institute for Sustainable Agriculture, Spanish National Research Council (IAS-CSIC), Av. Menéndez Pidal s/n, 14004 Córdoba, Spain; mjcobos@ias.csic.es (M.J.C.); cmruiz@ias.csic.es (C.M.R.-P.); diego.rubiales@ias.csic.es (D.R.)

² Programa de Doctorado de Ingeniería Agraria, Alimentaria, Forestal y de Desarrollo Rural Sostenible, Universidad de Córdoba, 14071 Córdoba, Spain

* Correspondence: majimenez@ias.csic.es

Abstract

Ascochyta blight remains a major constraint for field pea (*Pisum sativum* L.) production and a priority for breeding programmes. So far, only moderate levels of incomplete resistance have been identified in pea germplasm and accumulated in pea cultivars by breeding. Resistance identified so far appears to be of complex inheritance, with phenotypic expression strongly affected by plant phenology and morphology and by environmental factors. This has slowed down the development and release of resistant elite cultivars. In this work, we describe the development of novel resistant breeding lines derived from targeted intra- and interspecific crosses combined with cycles of selection under high disease pressure at seedling and adult plant stages. The performance of thirteen breeding lines selected for improved resistance and good agronomic traits was further validated in a comparative field trial. Results confirmed the successful combination of competitive yield and good standing ability with good levels of resistance exceeding those of the resistant check. These advanced breeding lines are available on request for research and breeding use.

Keywords: *Pisum sativum*; field pea; Ascochyta blight; breeding; germplasm; quantitative resistance; MGIDI

1. Introduction

Field pea (*Pisum sativum* L.) is one of the main temperate grain legumes, supplying protein for food and feed value chains and contributing to the resilience of cereal-based rotations through biological nitrogen fixation and related agroecosystem services [1,2]. Field peas are cultivated worldwide, occupying from 7.2 to 7.4 million ha with average grain yield ranging from 1.7 to 2.0 t ha⁻¹ considering the last 5-year period with available data (i.e., 2019–2023) [3]. Despite these advantages, pea production is often constrained by a small number of recurrent diseases that can destabilise yield and seed quality, with Ascochyta blight (typically expressed as necrotic spots on leaves and stems) remaining among the most significant [4–6]. Epidemics are strongly influenced by weather and can fluctuate widely between seasons, with disease development typically favoured by cool, wet conditions from flowering to pod development. In the field, Ascochyta blight is caused by a pathogen complex, most frequently involving *Didymella pinodes* (syn. *Peyronellaea pinodes*), *Didymella pinodella* (syn. *Peyronellaea pinodella*) and *Ascochyta pisi* (teleomorph



Academic Editors: Anders S. Carlsson and Yinghui Li

Received: 30 December 2025

Revised: 15 March 2026

Accepted: 23 March 2026

Published: 25 March 2026

Copyright: © 2026 by the authors. Licensee MDPI, Basel, Switzerland. This article is an open access article distributed under the terms and conditions of the [Creative Commons Attribution \(CC BY\)](https://creativecommons.org/licenses/by/4.0/) license.

Didymella pisi), while *Ascochyta koolunga* has been documented in Australian pea-growing regions [7]. Among them, *D. pinodes* appears to be the most aggressive and economically important [5,8–10]. This complexity also highlights the need for preventive management and breeding strategies that consider not only the species already present in a region but also those not yet detected locally that could be introduced and lead to future outbreaks [11–14]. Disease management relies on integrating host resistance with agronomic practices and fungicides, especially in wetter seasons [5,15,16]. Together, pathogen heterogeneity and weather effects on epidemics create a variable disease context that needs to be considered when studying resistance expression.

Against this background, genetic resistance remains the key to achieving stable crop protection. Resistance to the most damaging component of the pathogenic complex, *D. pinodes*, is quantitatively inherited and a number of quantitative trait loci (QTLs) have been identified [17–24]. Accordingly, breeding progress has relied on introgression and recombination of multiple minor-effect loci from diverse sources, particularly wild *Pisum* relatives and non-elite germplasm [4–6,17–25]. Germplasm screenings and subsequent genetic studies highlighted valuable sources of partial resistance to *D. pinodes* in *Pisum fulvum* and *Pisum sativum* subsp. *syriacum*, which have since supported QTL discovery and the design of resistance-enriched breeding backgrounds [22,25,26]. Recent work further supports the idea that resistance loci may be tightly linked to architectural or phenological traits, reinforcing the need to track resistance alongside these traits during selection [8,19,27,28]. However, despite substantial advances in QTL discovery and molecular resources, translating partial-resistance loci into broadly competitive, widely adopted cultivars remains slow, because their effects are modest and must be combined with agronomic adaptation under variable epidemic conditions.

In addition, the field expression of partial resistance is strongly influenced by canopy development and plant type, because architecture shapes plant microclimate and level of pathogen exposure, thereby affecting disease development. Lodged and dense canopies can increase within-canopy humidity and leaf wetness duration, amplifying infection [28–30]. Disease pressure translates into yield penalties through a reduction in green leaf area, assimilate supply and yield components, ultimately affecting partitioning efficiency [31]. While some genetic and epidemiological studies do record *Ascochyta* blight together with phenology, plant height, lodging and/or yield, notably in mapping populations [22,28], few reports extend this into decision-orientated assessments of advanced breeding lines that integrate disease response and key agronomic traits in a single, selection-relevant framework. As a result of all these factors, only moderate levels of resistance have been incorporated into cultivated backgrounds despite the huge breeding efforts worldwide [4,6,32–34].

In this context, we describe the development of advanced pea breeding lines derived from resistance-enriched pedigrees. The breeding lines assessed here derive from targeted crosses bringing together well-documented resistance sources and agronomically relevant parents, with subsequent iterative screening under controlled conditions and in the field to accumulate partial resistance. Response to *Ascochyta* blight was monitored after each cycle of selection, and a final validation trial was performed to check the level of resistance accumulated. Our study focused on *D. pinodes*, since it is the predominant pathogen in the region and the most widespread. We report the validation data providing an initial view of resistance levels achieved, together with the main agronomic traits that guide breeding decisions: standing ability, phenology and yield.

2. Materials and Methods

2.1. Development and Selection of Resistant Breeding Lines

The breeding lines described here represent four partially related breeding backgrounds (A–D, Table 1). Each of them derives from resistance-enriched pedigrees initiated

by a set of founding crosses (i.e., cumulative multi-parent crosses). Parental lines contributing to the founding crosses included locally adapted cultivars and in-house breeding lines [35,36], previously reported sources of partial resistance or tolerance to *D. pinodes* (Radley [37,38], Baccara [38,39], Pearl [24,40], OZP-1207 [41]) and wild *Pisum* accessions with demonstrated partial resistance (P665 [21,25,42,43], Pf660 [25]). Derived segregating populations were advanced by recurrent selection for resistance. Selection started at F2 already, combining selection for resistance under controlled conditions (CCs), ensuring high disease pressure, with field screenings under disease-prone conditions and stake support. The level of resistance of Radley was the reference threshold, retaining only the lines with higher resistance than Radley. After ≥ 4 selection cycles, progenies from certain founding crosses were also intercrossed (as described by [4]) to recombine resistance sources prior to further selection (Figure 1). Care was taken also to select only lines of the *afila* type, to improve standing ability.

Table 1. Summary of the pea genotypes evaluated in the trial, grouped by pedigree.

Genotype	Pedigree	Resistance Sources	Pedigree Group
56	[[Pearl × [(Ballet × P665) × Radley]] × [Kayanne × [B99-100 × [(Messire × Pf660) × Messire] × Ballet]] × (Toro × Baccara)] × [(Radley × Toro) × KI34]	Radley	A
57		Pearl	
59		Baccara	
63		P665 (<i>Pisum sativum</i> ssp. <i>syriacum</i>) Pf660 (<i>Pisum fulvum</i>)	
24	[[[(Ballet × P665) × Radley] × KI34] × [Pearl × (Radley × Toro)]]	Radley	B
28		Pearl	
29		Baccara	
34		P665 (<i>Pisum sativum</i> ssp. <i>syriacum</i>)	
38			
40			
75-1	[[AGT205,21 × [(Messire × Pf660) × Messire] × Ballet]] × OZP-1207] × [KI34 × (Radley × Toro)]	Radley	C
75-2		OZP-1207	
83	(Radley × Toro) × KI34	Radley	D
Radley			Resistant check
Messire			Susceptible check

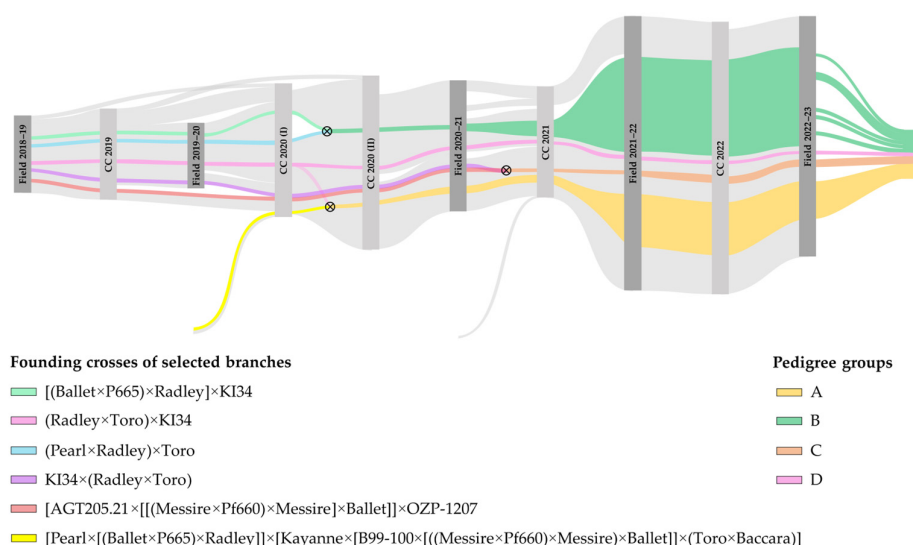


Figure 1. Alluvial diagram summarising the progression of pea breeding material (horizontal ribbons) through successive field and controlled condition (CC) selection stages from 2018 to 2022 (vertical

bars). Ribbon width is proportional to the number of lines sharing a pedigree at each stage. Coloured ribbons highlight the pedigree branches that generated the advanced lines evaluated in this study and their founding crosses, according to the legend. Cross symbols mark crossing events where material from two branches was combined to generate the subsequent breeding population. A more detailed guide to interpreting this figure is provided in Appendix A.

2.2. Validation Field Trial: Assessment of Disease and Agronomic Traits

The field validation trial of previously selected breeding lines was conducted during the 2023–2024 growing season at an experimental station in Córdoba, southern Spain, under Mediterranean rainfed conditions. All 15 genotypes (13 breeding lines + 2 check cultivars) were sown in 1 m² plots, using a seed density of 45 seeds m⁻². The experiment followed a Randomised Complete Block Design (RCBD) with three replicates per genotype. Plots were naturally infected by *Ascochyta* blight, with no artificial inoculation performed. High and spatially uniform disease pressure was ensured by bordering each plot on three sides by a strip of the susceptible cultivar Messire acting as a conidial spreader. Sowing was carried out in autumn, favouring early onset and sustained development of *Ascochyta* epidemics during the crop cycle. Overhead micro-sprinklers were used during a dry period in mid-spring to prolong leaf wetness, while during the rest of the cycle the crop grew under rainfed conditions. A pre-emergence herbicide application (45% pendimethalin) was applied, with no additional phytosanitary treatments.

Disease severity (*DS*) was assessed once per plot towards the end of the crop cycle, before the onset of senescence. *DS* was visually estimated as the percentage of total aerial biomass within the plot showing *Ascochyta* blight lesions. This trait was assessed by a trained team, including the lead rater who had also conducted the disease scorings in the preceding selection stages of the programme, thereby ensuring a common stable criterion. This single late assessment provided the final disease level of each plot within the trial. Flowering onset was monitored throughout the cycle as a phenological earliness indicator. For each plot, the onset of flowering was defined as the date when 50% of plants had opened their first flower. Growing Degree Days to flowering (*Flowering GDD*) were then calculated from sowing to that date, using local daily temperature records retrieved from the 'Red de Información Agroclimática de Andalucía' database [44] and considering a base temperature of 3 °C. *Lodging* was scored once at the end of the crop cycle after maximum canopy development. It was rated on a 1–10 scale, where 1 corresponded to completely erect plots (approximately 90° stem angle relative to the ground) and 10 to fully lodged canopies. At harvest, the total weight of above-ground dry biomass per plot was recorded, and grain dry weight was determined after mechanical threshing. These measurements were used to calculate relative grain yield (*rGY*), as the fold change in grain yield relative to the mean yield of the resistant check Radley within the trial. The Harvest Index (*HI*) was computed as the percentage ratio of grain dry weight to total above-ground dry biomass.

2.3. Traits Modelling

Agronomic, phenological and disease-related traits were modelled at the plot level to obtain both variance components and adjusted genotype means under the field design. All the models were fitted in R software (v. 4.3.3.) [45]. Block was treated as a design-related fixed effect under two alternative models. First, a linear mixed model (LMM) was specified as

$$Y_{ij} = \mu + B_j + g_i + \varepsilon_{ij}, \quad (1)$$

where Y_{ij} is the plot value of the trait for genotype i in Block j , B_j is the fixed effect of the block, $g_i \sim N(0, \sigma_g^2)$ is the random effect of the genotype, and $\varepsilon_{ij} \sim N(0, \sigma_e^2)$ is the

residual error. LMMs were fitted by Restricted Maximum Likelihood (REML) using the packages ‘lme4’ (v. 1.1.37) and ‘lmerTest’ (v. 3.1.3) [46,47] assuming independent, normally distributed residuals. From the estimated variance components (i.e., the genotypic σ_g^2 and the residual σ_e^2 variances), a within-trial broad-sense heritability (h^2) on an entry mean basis was estimated as

$$h^2 = \frac{\sigma_g^2}{\sigma_g^2 + \sigma_e^2 / r}. \quad (2)$$

In parallel, a linear fixed-effects model (LM) was also fitted by ordinary least squares, and genotype means were extracted with the ‘emmeans’ R package (v. 1.11.2.8) [48]. For all the traits, Genotype (G_i) and Block (B_j) were included as fixed effects,

$$Y_{ij} = \mu + G_i + B_j + \varepsilon_{ij}. \quad (3)$$

Genotype means were then obtained as Estimated Marginal Means (EMMs), here equivalent to Best Linear Unbiased Estimators (BLUEs). The resulting genotype \times trait matrix of BLUEs for DS, Lodging, Flowering GDD, rGY and HI was used as the input for the multivariate analyses.

2.4. Trait Correlations and Principal Component Analyses

Relationships among traits were explored at the genotype level using the design-adjusted BLUEs described in Section 2.3. Pairwise associations between traits were quantified using Pearson correlation coefficients computed from the genotype \times trait BLUE matrix. Pearson’s r was computed in R software (v.4.3.3) [45] using the ‘cor()’ function (method = “pearson”), from the observations across genotypes for the traits involved.

Principal component analysis (PCA) was then applied to the same matrix in order to summarise multi-trait patterns of variation. Before PCA, each trait was centred and scaled to unit variance (i.e., z-scores). PCA was performed in R software with ‘prcomp()’ (center = TRUE, scale. = TRUE) on the genotype \times trait BLUE matrix. The proportion of variance explained by each principal component was obtained from the corresponding eigenvalues. The variance captured by the addition of successive components was inspected, and the first two components were retained for a PC1–PC2 biplot representation with trait loadings visually overlaid as vectors.

2.5. Multi-Trait Selection

Multi-trait genotype selection was performed using the multi-trait genotype–ideotype distance index (MGIDI) implemented in ‘metan’ R package (v. 1.19.0) [49]. The input data for MGIDI were the design-adjusted BLUEs described in Section 2.3. As an ideotype reference, lower values were defined as desirable for the traits *DS*, *Lodging* and *Flowering GDD*, and higher values as desirable for *HI* and *rGY*. The MGIDI was computed according to the standard procedure described by Olivoto and Nardino [50]: trait values are first rescaled according to the ideotype vector, then a factor analysis is carried out on the trait correlation matrix, and finally the Euclidean distance between each genotype and the ideotype is calculated in the space of the retained factors. The number of retained factors followed the default criterion implemented in ‘metan’ (minimum eigenvalue for retention, ‘mineval = 1’), and factor loadings were rotated using the varimax criterion.

Trait weights were incorporated into the MGIDI calculation to shape it. First, we used h^2 estimated from LMMs according to Equation (2). Thus, baseline weighting for each trait was computed by dividing each h^2 value by the mean h^2 across traits to obtain a heritability-based weight vector. Two additional weighting schemes were then considered

to complement it. For a “Balanced scheme”, all traits were assigned the same multiplicative factor ($w = 1$) and renormalised to centre their mean. Alternatively, a “Resistance–yield emphasis scheme” was designed, for which *DS* and *rGY* were given a $w = 2$ factor before renormalisation, while the rest of the traits retained a $w = 1$.

3. Results

3.1. Field Performance, Resistance and Agronomic Traits

All breeding lines were *afila* type, although the parental lines involved in the crosses differed in leaf type. Parentals P665, Pf660, Toro and Messire had “normal” leaves, whereas Radley, Pearl, Ballet, Baccara, KI34, AGT205 and OZP-1207 were *afila*. This indicates effective selection for the trait.

The stress-test design effectively generated high *Ascochyta* blight pressure. Disease severity (*DS*) at plot level ranged from 20 to 90% canopy area affected, with a trial mean of 55.1% (Table 2). This confirms that the trial operated under severe and highly informative disease conditions. Growing Degree Days to flowering (*Flowering GDD*) ranged from 752 to 1051 °C days, with a mean of 968 °C days, and one markedly earlier genotype strongly conditioning this metric (Messire, below 800 °C days). Grain yield relative to Radley (*rGY*) exhibited the largest dispersion, ranging from 0.16 to 1.66 relative to the resistant check Radley.

Table 2. Descriptive statistics and broad-sense heritability for the assessed traits.

Trait		Mean	SD	CV	min.	max.	h^2
<i>DS</i>	(% canopy affected)	55.13	19.52	35.4	20	90	0.828
<i>Flowering GDD</i>	(°C days)	967.91	65.5	6.77	752	1051	0.848
<i>rGY</i>	(× fold Radley yield)	0.76	0.44	0.58	0.16	1.66	0.965
<i>HI</i>	(% grain dry weight)	18.36	7.73	42.09	3.9	36.4	0.746
<i>Lodging</i>	(1–10 scale)	5.89	2.07	35.14	2	9	0.846

Broad-sense heritabilities on an entry mean basis (h^2) were high for all traits. *Flowering GDD* showed the highest heritability, consistent with a very stable expression of phenology across blocks. *DS*, *rGY* and *Lodging* also displayed high heritabilities (Table 2). These estimates indicate that most of the observed between-genotype variation for these traits is attributable to genetic differences rather than plot-level noise and support their use as primary criteria in the subsequent multi-trait evaluation.

3.2. Trait Associations Revealed by Correlations and Principal Component Analysis

Pearson correlations among design-adjusted BLUEs (Best Linear Unbiased Estimators) revealed a coherent pattern of associations between disease, agronomic and phenological traits (Figure 2). *DS* was strongly positively correlated with *Lodging* ($r = +0.73$), indicating that more lodged canopies tended to be more diseased. *DS* was also strongly negatively correlated with *Flowering GDD* ($r = -0.75$), suggesting lower disease in later-flowering genotypes, in line with previous reports that highlight the flowering-to-maturity phase as a main susceptibility window for epidemic development [5,22]. Because Messire is an intentionally extreme, markedly early, lodging-prone, susceptible check, we assessed whether these relationships were primarily driven by this single genotype. Excluding Messire reduced the magnitude of the *DS–Flowering GDD* association, but it remained negative ($r = -0.62$), while the *DS–Lodging* correlation changed only slightly ($r = +0.68$). The latter indicates that the *DS–Lodging* correlation is not driven solely by Messire’s extreme architecture and remains substantial among

the *afila* genotypes, pointing to standing ability per se as an important contributor to disease expression.

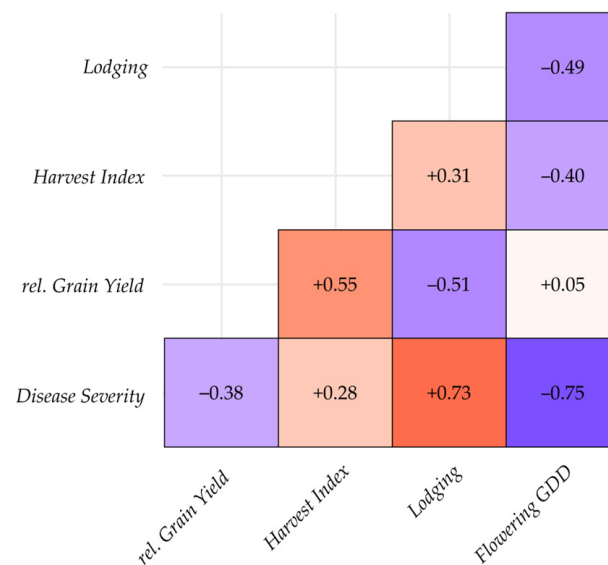


Figure 2. Pearson correlation heatmap among disease, agronomic and phenological traits based on design-adjusted BLUEs (Best Linear Unbiased Estimators). Cell colour indicates Pearson's r value (warm colours = positive; cool colours = negative; colour intensity proportional to $|r|$). The corresponding r value is shown in each cell.

The association between DS and rGY was negative but only moderate ($r = -0.38$). Nevertheless, the relationship between these two traits merits a more detailed examination in order to resolve genotype-specific performance patterns within this negative association. Figure 3 offers a genotype-level view of this pair of traits, allowing the phenotype of each breeding line to be evaluated on its own merits, while also illustrating the overall negative trend (it must be noted the absence of genotypes combining high DS with high rGY in this panel). The susceptible check Messire occupied the most unfavourable region of the plot (bottom-right quadrant), confirming its role as a susceptible standard. Breeding lines 75-1 and 75-2 also combined high DS with moderate or low yields. In contrast, several breeding lines (i.e., 28, 38, 57 and 29) grouped in the favourable area of DS near or below resistant Radley and rGY above it, indicating that improved disease response can be combined with competitive yield under severe infection pressure. Other lines, such as 56, 59 and 63, displayed relatively low DS but rGY substantially below the trial mean, illustrating the diversity of phenotype profiles generated and selected within this programme. The dispersion of plot-level observations is summarised in Figure 3 by the ellipses drawn around each genotype, representing its median absolute deviation (MAD) along each axis. Apart from a few highly balanced cases (most notably breeding line 38, which showed very limited dispersion for both traits), there is a tendency for the most resistant genotypes (e.g., lines 28 and 57 and Radley) to display larger deviations from their mean DS , while still maintaining clearly discernible behaviours. In more susceptible genotypes, DS tended to be more stable across replicates, and their phenotypic variability was dominated by differences in rGY , which may reflect a stronger sensitivity of pod filling efficiency to adverse environmental conditions. In any case, these associations are not interpreted as causal effects but as selection-relevant patterns within this advanced panel under a stringent stress-test context.

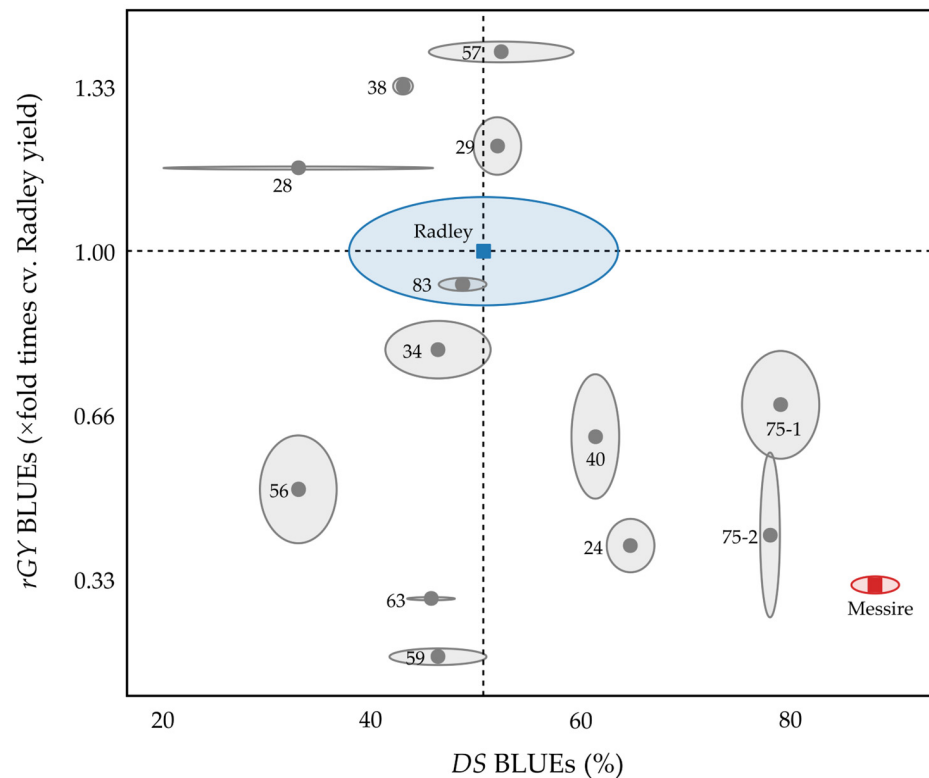


Figure 3. Relationships between design-adjusted BLUEs (Best Linear Unbiased Estimators) for grain yield relative to Radley (rGY) and Ascochyta blight disease severity (DS) for all genotypes of this validation trial. Dashed lines mark the reference values of the resistant check Radley, which define four quadrants. The check cultivars Messire and Radley are shown as red and blue squares, respectively. Each genotype is represented by a grey point surrounded by an ellipse defined by the median absolute deviation (MAD) along each trait, computed as the median of the absolute deviations of the adjusted per-replicate values from median. These MAD ellipses are descriptive summaries of within-genotype dispersion and do not represent confidence intervals or regions.

Principal component analysis (PCA) of the standardised BLUE matrix summarised these relationships in a low-dimensional trait space (Figure 4). The first principal component (PC1) accounted for 50.2% of the total variance and was driven primarily by DS and *Lodging* loading in the same direction, with *Flowering GDD* loading in the opposite. PC1 therefore describes a major gradient from early, lodged and more diseased genotypes to later, better-standing and less diseased ones. The second principal component (PC2) explained an additional 32.5% of the variance and was mainly associated with rGY and *HI* (moderately correlated with each other, according to their Pearson's $r = 0.55$). Considering the relative positions of each genotype within the PCA space, Messire appeared clearly separated from the rest of the panel along the unfavourable direction mainly defined by high DS and *Lodging* and its previously mentioned phenological earliness. A group of susceptible breeding lines (i.e., 75-1, 75-2, 24 and 40) projected towards this unfavourable sector, consistent with their high *Lodging* scores (BLUEs ranging from ~ 7.3 to 8.7), which likely contributed to the resulting high disease severity. Check Radley was located close to the origin but shifted towards the direction of lower DS . Several breeding lines (notably 38, 57, 29 and 28) clustered in a more favourable region of the space, combining moderate or low DS and *Lodging* with a clearly higher rGY and *HI*. The PC1–PC2 biplot also reveals some pedigree-related structuring of the material. Although the number of lines per pedigree group is limited and unbalanced, some clustering patterns can be observed alongside the PCA space for breeding lines sharing genetic background. This would indicate that multi-trait profiles are not randomly distributed across genetic backgrounds and that specific

founder combinations may have actively guided some of the breeding lines towards the most promising phenotypic profiles.

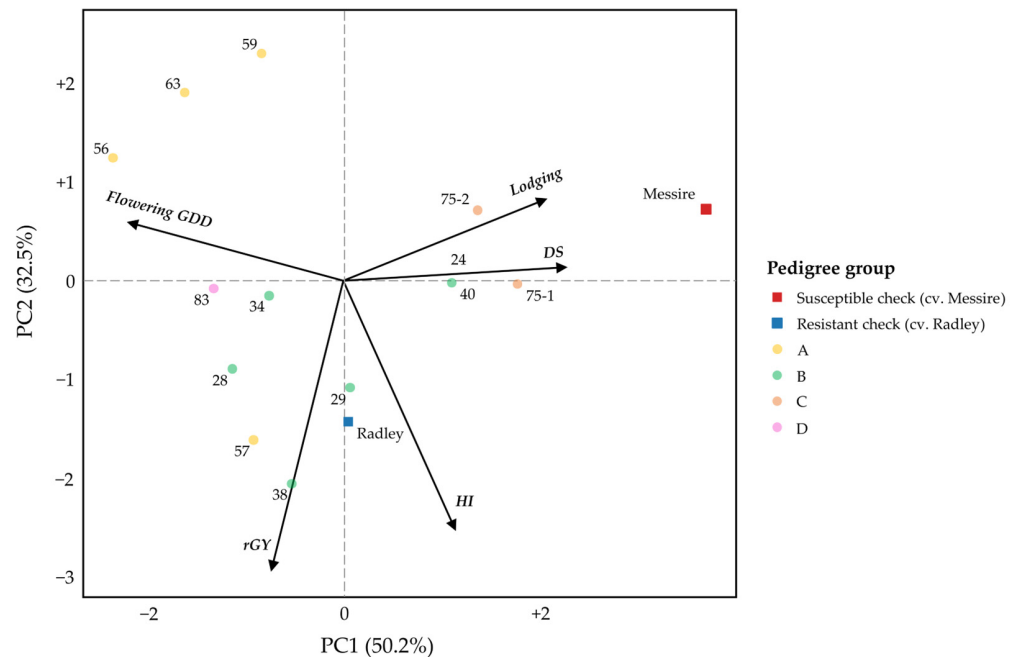


Figure 4. Principal component biplot (PC1 vs. PC2) based on standardised design-adjusted BLUEs (Best Linear Unbiased Estimators) for the assessed traits. Traits are shown as vectors indicating the magnitude and direction of their loadings, while genotypes are plotted according to their PC1–PC2 scores, with Messire (red square) and Radley (blue square) as check references and breeding lines coloured by pedigree group.

3.3. Integrative Multi-Trait Assessment of Breeding Lines with MGIDI

The multi-trait genotype–ideotype distance index (MGIDI) was used to rank genotypes according to their overall performance for the traits assessed in this trial. Broad-sense heritabilities (Table 2) were used as baseline weights so that traits with a stronger genetic signal contributed more to the index than traits with greater residual variation. This weighting makes the index closer to a multi-trait genetic merit score than a simple phenotypic desirability measure. In this way, MGIDI provides a transparent prioritisation tool for advanced material under the field conditions used for validation.

Under the “Balanced scheme”, where only the h^2 baseline weights were applied, MGIDI values showed a wide spread among genotypes. When the “Resistance–yield emphasis scheme” was computed with *DS* and *rGY* doubled relevance within the index calculation (Figure 5), the overall MGIDI range shifted slightly, but the ranking remained highly consistent. Importantly, the same five genotypes (i.e., 38, 57, Radley, 28 and 29) still occupied the top positions, although their internal order changed between these two operative schemes: line 38 remained the best, now followed by 57, Radley, 28 and 29. At the lower end, Messire proved the worst-ranked genotype, whereas lines 59 and 63 also retained very poor MGIDI scores. This stability of the top five set across schemes indicates that the selection of better crop profiles is robust to reasonable changes in trait weighting. Notably, the highest-ranked breeding lines consistently include genotypes that match or surpass the resistant check while maintaining competitive productivity under severe disease pressure.

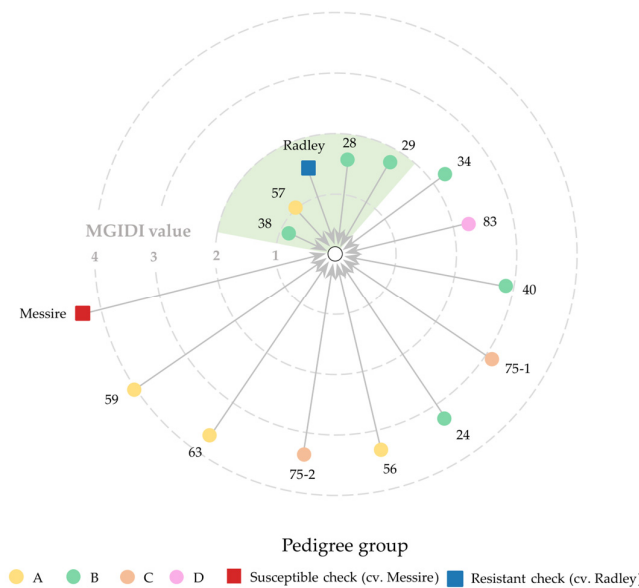


Figure 5. Multi-trait genotype–ideotype distance index (MGIDI) for the studied pea genotypes under the “Resistance–yield emphasis scheme”. The ideotype is shown as a white circle. Genotypes (coloured by pedigree group) are plotted by their overall distance to the ideotype (grey arrows; shorter distances are more desirable). The susceptible check Messire and the resistant check Radley are shown as red and blue squares, respectively. Concentric dashed rings mark the numerical reference for MGIDI values (indicated by the grey the number inserted into each ring). The green-shaded sector outlines the five top-ranked genotypes.

The profile of the best MGIDI lines illustrates different ways of achieving multi-trait superiority, which can be appreciated by inspecting the BLUE values for each trait summarised in Figure S1. Line 38 combines relatively low disease susceptibility and excellent relative yield with *HI*, *Lodging* and phenology in a desirable range, explaining its consistently outstanding MGIDI. Line 57 achieves very high relative yield and remarkably standing ability, but with mean disease resistance not exceeding that of Radley. The high-ranking position achieved by this genotype reflects the fact that, under the MGIDI schemes designed for this validation trial, a good yielding capacity can elevate a genotype’s score even when resistance gains are moderate, benefitting from the stronger basal weight of *rGY* through its higher h^2 . Lines 28 and 29 are more resistant to *Ascochyta* blight than Radley; they are good yielders and maintain acceptable standing ability, offering a balanced improvement in resistance with no apparent yield sacrifice.

On this basis, lines 38, 57, 28 and 29 can be considered the best breeding lines emerging from the MGIDI analysis, with Radley retained as a useful reference rather than a target. Supplementary radar plots comparing these four candidates with the check genotypes (Figure S2) visually highlight how the selected lines approach the multi-trait ideotype.

4. Discussion

Ascochyta blight remains one of the major constraints to field pea production, consistently featuring among the top priorities of breeding programmes and integrated disease management strategies for this crop [4–6,51]. The present study was designed to validate agronomic performance under field conditions of breeding lines selected over a number of selection cycles. The stress-test framework was deliberately designed to emulate high disease pressure scenarios to place the evaluated material within a broader disease context. Our results highlight the value of both components of the germplasm obtained: on one hand, a small set of lines with balanced multi-trait profiles and competitive yield potential that merit consideration as breeding material for near-term use; on the other hand,

genetic backgrounds enriched in stacked resistance sources that can continue to sustain the breeding strategy.

Resistance to the *Ascochyta* blight complex in peas is incomplete and quantitative: multiple sources of partial resistance have been identified in landraces and in wild *Pisum* spp. germplasm [6], but no commercial cultivar exhibits strong resistance. The underlying resistance is governed by multiple quantitative trait loci (QTL) of modest effect [8,17–26,37], and their phenotypic expression is strongly modulated by the environment and microclimate [6,52] and affected by plant phenology and morphology [28–30]. Despite extensive genetic research and marker resources, converting partial-resistance features into consistently competitive field performance still relies on iterative resistance accumulation and validation schemes [4,53]. In this context, our hybridisation strategy was explicitly designed to broaden the genetic basis of resistance by combining multiple cultivated and wild partially resistant sources within pedigrees through cumulative crosses. This increases opportunities for recombination and accumulation of complementary minor-effect loci while reducing reliance on any single resistance source. This study shows the successful simultaneous improvement of *Ascochyta* blight resistance and agronomic value by recurrent selection under high disease pressure, which agrees with previous successful works [4,53].

Notably, a subset of breeding lines combined disease resistance surpassing Radley with very competitive yields. The MGIDI (multi-trait genotype–ideotype distance index) methodology formalised this multi-trait perspective while avoiding some limitations of classical linear selection indices [50] and supporting integrated improvement across agronomic and stress-response traits [54]. In our panel, the index consistently singled out the same five genotypes as top-ranked (i.e., breeding lines 38, 57, 28, 29 and Radley) under two alternative operative schemes. Within this set, line 38 represents the most balanced profile, combining high disease resistance with excellent relative yield and low lodging, whereas lines 28 and 29 benefit from good but not extreme relative yield, and line 57 stands out for its very high relative yield and standing ability. Conversely, lines 56, 34 and 83 showed comparatively good disease resistance yet ranked lower because of their poorer agronomic profiles. These genotypes therefore remain plausible resistance donors, particularly if future recombinations can decouple resistance to *Ascochyta* blight from unfavourable standing ability and/or phenology (traits that may influence in turn the field expression of the stacked resistance loci).

The pattern of expression of *Ascochyta* blight resistance in our trial can be partially interpreted in terms of canopy architecture and the quantitative nature of resistance. The role of lodging in aggravating *Ascochyta* blight infection in pea is well documented [4,29,30,53,55]. Plant architecture can modulate the spatio-temporal infection dynamics and splash dispersal within the canopy [28,56]. In line with this, disease severity (*DS*) was strongly correlated with *Lodging* across genotypes. The relatively high *DS* observed on some breeding lines (notably 75-1, 75-2, 24 and 40) illustrates this point: these genotypes had progressed through earlier selection stages, including controlled conditions and field screenings where plants were supported, but expressed weak standing ability when evaluated under more realistic field conditions, probably leading to their susceptible phenotypes. This underscores how canopy-related traits can condition the field expression of partial resistance. Leaf type is a major determinant of standing ability and can also influence *Ascochyta* blight development through canopy structure and microclimate [57]. The persistence of the *DS*–*Lodging*-negative correlation after excluding the normal-leaf check (Messire) indicates that standing ability is also a key driver of disease severity variation among *afila*-type genotypes. Phenology also emerged as an associated dimension, with earlier-flowering genotypes tending to show higher final disease severity, consistent with reports in pea and related grain legume pathosystems [22,58].

The genetic backgrounds of breeding lines evaluated in this work rely on a set of well-documented sources of incomplete resistance, crossed with advanced lines and adapted cultivars. These include wild relatives such as P665 (*Pisum sativum* subsp. *syriacum*) [8,42,43] and Pf660 (*P. fulvum*) [18], as well as pea varieties such as Radley, Baccara, Pearl or the breeding line OZP-1207 [37–42]. Overlaying the multi-trait profiles with the genealogical information provides a tentative picture of how parental combinations translated into field performance under severe disease pressure. Backgrounds incorporating the P665-derived resistance source together with Radley and adapted cultivar parents (i.e., pedigree background B) generated several of the best-balanced profiles (e.g., breeding lines 28, 29 and 38). Contrasting outcomes within this same background (i.e., 24 and 40) highlight the importance of standing ability and related agronomic traits in conditioning resistance expression from these sources. Background A, which incorporates Pf660 alongside other resistance sources and cultivated parents, produced strongly contrasting fixed lines, from poor agronomic profiles to an outstanding recombinant (line 57). This suggests that similar resistance-enriched backgrounds can still yield favourable combinations. By contrast, the lines derived from OZP-1207 (i.e., 75-1 and 75-2) underperformed in this Mediterranean stress test despite also carrying Radley as a parent; their alignment with high lodging and high disease severity is consistent with canopy-related exposure effects as previously discussed, and their behaviour is also compatible with the context dependence of resistance components across pathogen populations and cultivation environments [7,59,60]. More broadly, the absence of additional wild resistance sources within genetic background C may have limited opportunities for stacking complementary minor-effect loci relative to other pedigrees. These trends should be viewed as indicative rather than conclusive but are consistent with the expectation that stacking multiple sources of partial resistance can lead to strongly resistant profiles when combined with a high selection pressure framework.

Taken together, this single-environment stress-test evaluation provides a first picture of how our advanced lines perform under severe *Ascochyta* blight pressure and underlines the value of the germplasm generated. Further multi-environment validation is required to confirm stability and quantify genotype-by-environment effects on resistance expression. In parallel, expanding the resistance base from global germplasm collections [34,60], together with optimised phenotyping [61], marker-informed selection through novel molecular markers [26,27,62–64] and genomic selection [65], will make it more feasible to accumulate complementary minor-effect loci [66]. Against this agenda, our results show that high-pressure screening, combined with design-adjusted trait estimation and multi-trait selection, provides a practical breeding-decision framework for quantitative, environment-sensitive resistance traits such as *Ascochyta* blight disease. Moreover, they underscore the value of combining planned resistance-enriched crosses with stringent screening steps. This integrated approach enabled us to obtain and identify advanced lines in which multiple partial-resistance sources have been effectively stacked, resulting in improved resistance with competitive field performance under severe disease pressure. Importantly, this helps address a current gap in pea breeding: the limited availability of agronomically competitive material combining diverse resistance sources. This germplasm can now be shared and further tested across programmes and environments.

5. Conclusions

This study reports the development of advanced field pea germplasm from *Ascochyta* blight resistance-enriched pedigrees combining multiple sources of partial resistance with agronomically adapted backgrounds. When tested under deliberately severe *Ascochyta* blight pressure, this material expressed clear improvements over the resistant commercial

standard, with several breeding lines combining high resistance with good to acceptable standing ability and competitive yield.

Our results are also consistent with the role of canopy architecture and phenology in shaping field disease expression, supporting their relevance when interpreting resistance and defining selection priorities under field conditions. An integrated multi-trait evaluation enabled the identification of a small set of lines with a favourable resistance–performance balance, while also highlighting additional lines with low disease severity but less competitive overall agronomic profiles that may still be useful within breeding pipelines.

Overall, this work provides evidence that the resistance-enriched pedigrees developed can extend the range of effective resistance currently available to pea breeding. In addition to describing the development of these breeding lines, their resistance and agronomic value were validated under field conditions. The novel breeding lines described here constitute a valuable resource for further research and breeding efforts and can be made available on request for use by the wider research and breeding community. Testing these lines in other programmes elsewhere will also help to discern genotype-by-environment effects in multi-environment trials.

Supplementary Materials: The following supporting information can be downloaded at: <https://www.mdpi.com/article/10.3390/agriculture16070726/s1>, Figure S1: EMM/BLUE values at the genotype level for the variables assessed in the field validation, coloured according to breeding desirability (green = best; orange = worst); Figure S2: Phenotypic profiles of the top-MGIDI breeding lines and check lines, defined by the EMMs/BLUEs of the assessed variables (direction transformed in terms of breeding desirability); reference values being the most favourable (outer circle) and least favourable (centre) values observed in the set of genotypes.

Author Contributions: Conceptualisation, M.A.J.-V., M.J.C. and D.R.; methodology, M.A.J.-V.; software, M.A.J.-V.; validation, M.A.J.-V. and D.R.; formal analysis, M.A.J.-V.; investigation, M.A.J.-V., M.J.C., C.M.R.-P. and D.R.; resources, M.A.J.-V., M.J.C., C.M.R.-P. and D.R.; data curation, M.A.J.-V. and M.J.C.; writing—original draft preparation, M.A.J.-V.; writing—review and editing, D.R.; visualisation, M.A.J.-V.; supervision, D.R.; project administration, D.R.; funding acquisition, D.R. All authors have read and agreed to the published version of the manuscript.

Funding: This research was funded by the EU Horizon Europe COUSIN (grant number 101135314) and BELIS (grant number 101081878); by Spanish projects CPP2022-009742, PID2023-146215OB-I00 (MICIU/AEI/10.13039/501100011033) and by the FPU programme (grant number FPU20/04024) (MICIU/10.13039/100014440).

Data Availability Statement: The original data presented in this study are openly available in DIGITAL.CSIC at <https://doi.org/10.20350/digitalCSIC/17867> (accessed on 1 December 2025).

Conflicts of Interest: The authors declare no conflicts of interest.

Abbreviations

The following abbreviations are used in this manuscript:

QTL/QTLs	Quantitative trait loci
IAS-CSIC	Institute for Sustainable Agriculture (Spanish National Research Council)
CCs	Controlled conditions
RCBD	Randomised Complete Block Design
DS	Disease severity
GDD	Growing Degree Days
rGY	Grain yield relative to Radley
HI	Harvest Index
REML	Restricted Maximum Likelihood
LMM	Linear mixed models

LMS	Linear (fixed effects) models
EMMs	Estimated Marginal Means
BLUES	Best Linear Unbiased Estimators
PCA	Principal component analysis
PC1/PC2	First/second principal components
MAD	Median absolute deviation
MGIDI	Multi-trait genotype–ideotype distance index
h^2	Broad-sense heritability (entry mean basis)
QTL/QTLs	Quantitative trait loci
IAS-CSIC	Institute for Sustainable Agriculture (Spanish National Research Council)
CC	Controlled-Conditions
RCBD	Randomised Complete Block Design
DS	Disease Severity
GDD	Growing Degree Days
r_{GY}	Grain Yield relative to Radley
HI	Harvest Index
REML	Restricted Maximum Likelihood
LMM	Linear mixed models
LM	Linear (fixed-effects) models
EMMs	Estimated Marginal Means
BLUES	Best Linear Unbiased Estimators
PCA	Principal Component Analysis
PC1/PC2	First/second Principal Components
MAD	Median absolute deviation
MGIDI	Multi-trait genotype–ideotype distance index
h^2	Broad-sense heritability (entry mean basis)

Appendix A. Guide to Interpreting Figure 1

Figure 1 summarises the selection history of pea breeding material in the IAS-CSIC programme across successive screening stages from 2018 to 2022 using an alluvial diagram. The diagram should be read from left to right following the chronological sequence of stages. Vertical bars represent discrete selection events conducted either in the field (“Field”) or under controlled conditions (“CC”). Horizontal ribbons represent cohorts of breeding material sharing a common pedigree as they progress through these stages.

Ribbon width and continuity. Ribbon width is proportional to the number of breeding lines represented by a given pedigree cohort at a given stage. As material is advanced or discarded between stages, ribbons may narrow or disappear (removal from the programme). Conversely, widening reflects the expansion of a pedigree cohort due to the production of a larger number of progeny-derived lines at the preceding stage, which were then carried forward for testing in the subsequent stages. Grey ribbons depict breeding material that was screened in the programme but was not ultimately carried forward to the set of advanced lines evaluated in the present study.

Colour coding and founding crosses. Coloured ribbons highlight the pedigree cohorts that ultimately generated the advanced breeding lines evaluated in the field validation trial reported here. Colour codes have been assigned to these pedigree cohorts and to the founding crosses listed in the legend (which indicate the initial pedigree combinations from which each highlighted cohort originates). For clarity, only the cohorts relevant to the advanced lines retained for field validation are colour-emphasised; other material is displayed in grey to provide programme context.

Crossing events. Cross symbols (⊗) indicate explicit crossing events where breeding material from two distinct pedigree branches was combined to generate a new population that then entered subsequent selection stages. In these cases, two ribbons converge at the

symbol location and a single ribbon continues forward, representing the newly created hybrid-derived population. The position of the ⊗ symbol therefore marks the stage at which the cross was made within the programme timeline.

Timing of screening stages. Field stages correspond to cropping cycles defined by sowing and harvest, whereas CC stages correspond to screening periods conducted within a given calendar year. The approximate timing of each stage shown in Figure 1 is as follows:

- Field 2018–19: sown autumn 2018; harvested late spring 2019.
- CC 2019: early summer 2019.
- Field 2019–20: sown late summer 2019; harvested early winter 2020.
- CC 2020 (I): winter 2020.
- CC 2020 (II): early autumn 2020.
- Field 2020–21: sown late autumn 2020; harvested late spring 2021.
- CC 2021: summer 2021.
- Field 2021–22: sown autumn 2021; harvested late spring 2022.
- CC 2022: summer 2022.
- Field 2022–23: sown autumn 2022; harvested late spring 2023.

Relationship to the validated material. The right-hand side of the diagram represents the final stages of field and controlled-condition selection immediately preceding the 2023–2024 plot-scale field validation described in this study. The coloured cohorts reaching these later stages correspond to the pedigrees of the 13 advanced breeding lines included in the validation trial (Table 1).

References

1. Cernay, C.; Pelzer, E.; Makowski, D. A global experimental dataset for assessing grain legume production. *Sci. Data* **2016**, *3*, 160084. [CrossRef]
2. Rawal, V.; Navarro, D.K. (Eds.) *The Global Economy of Pulses*; Food and Agriculture Organization of the United Nations: Rome, Italy, 2019. [CrossRef]
3. Food and Agriculture Organization of the United Nations. FAOSTAT Statistical Database. Available online: <https://www.fao.org/faostat/> (accessed on 2 July 2025).
4. Adhikari, K.N.; Khan, T.N.; Stefanova, K.; Pritchard, I. Recurrent breeding method enhances the level of blackspot (*Didymella pinodes* (Berk. & Blox.) Vestergr.) resistance in field pea (*Pisum sativum* L.) in southern Australia. *Plant Breed.* **2014**, *133*, 508–514. [CrossRef]
5. Khan, T.N.; Timmerman-Vaughan, G.M.; Rubiales, D.; Warkentin, T.D.; Siddique, K.H.M.; Erskine, W.; Barbetti, M.J. *Didymella pinodes* and its management in field pea: Challenges and opportunities. *Field Crops Res.* **2013**, *148*, 61–77. [CrossRef]
6. Rubiales, D.; Barilli, E.; Rispaïl, N. Breeding for biotic stress resistance in pea. *Agriculture* **2023**, *13*, 1825. [CrossRef]
7. Fonseka, D.L.; Markell, S.G.; Zaccaron, M.L.; Ebert, M.K.; Pasche, J.S. Ascochyta blight in North Dakota field pea: The pathogen complex and its fungicide sensitivity. *Front. Plant Sci.* **2023**, *14*, 1165269. [CrossRef]
8. Zhang, R.; Hwang, S.-F.; Gossen, B.D.; Chang, K.-F.; Turnbull, G.D. A quantitative analysis of resistance to *Mycosphaerella Blight* in field pea. *Crop Sci.* **2007**, *47*, 162–167. [CrossRef]
9. Gossen, B.D.; Hwang, S.F.; Conner, R.L.; Chang, K.F. Managing the Ascochyta blight complex on field pea in Western Canada. *Prairie Soils Crops* **2011**, *4*, 135–141.
10. Tivoli, B.; Banniza, S. Comparison of the epidemiology of Ascochyta blights on grain legumes. *Eur. J. Plant Pathol.* **2007**, *119*, 59–76. [CrossRef]
11. Onfroy, C.; Tivoli, B.; Corbière, R.; Bouznad, Z. Cultural, molecular and pathogenic variability of *Mycosphaerella pinodes* and *Phoma medicaginis* var. *pinodella* isolates from dry pea (*Pisum sativum*) in France. *Plant Pathol.* **1999**, *48*, 218–229. [CrossRef]
12. Owati, A.; Agindotan, B.; Burrows, M. Characterization of fungal species associated with Ascochyta blight of dry pea in Montana and North America and development of a differential medium for their detection. *Plant Health Prog.* **2020**, *21*, 262–271. [CrossRef]
13. Tran, H.S.; Li, Y.P.; You, M.P.; Khan, T.N.; Pritchard, I.; Barbetti, M.J. Temporal and spatial changes in the pea Black spot disease complex in Western Australia. *Plant Dis.* **2014**, *98*, 790–796. [CrossRef] [PubMed]
14. Annan, E.N.; Mwanza, C.; Lucas, B.; Yan, Q.; Huang, L. Interspecific interactions and host background influence the population dynamics of the species causing the Ascochyta blight complex in pea. *Plant Pathol.* **2025**, *74*, 1878–1890. [CrossRef]

15. McDonald, G.K.; Peck, D. Effects of crop rotation, residue retention and sowing time on the incidence and survival of ascochyta blight and its effect on grain yield of field peas (*Pisum sativum* L.). *Field Crops Res.* **2009**, *111*, 11–21. [[CrossRef](#)]
16. Gudero Mengesha, G.; Terefe, H.; Yae, A.J.; Arato, A.A.; Betire, M.G.; Shago, T.S.; Bires, Z.F.; Borano, B.B.; Abebe, S.M. Integration of host resistance and fungicides reduced ascochyta blight pressure and minimised yield loss in field pea (*Pisum sativum* L.) in southern Ethiopia. *Acta Agric. Scand. B Soil Plant Sci.* **2022**, *72*, 971–986. [[CrossRef](#)]
17. Timmerman-Vaughan, G.M.; Frew, T.J.; Russell, A.C.; Khan, T.; Butler, R.; Gilpin, M.; Murray, S.; Falloon, K. QTL mapping of partial resistance to field epidemics of Ascochyta blight of pea. *Crop Sci.* **2002**, *42*, 2100–2111. [[CrossRef](#)]
18. Tar'an, B.; Warkentin, T.; Somers, D.J.; Miranda, D.; Vandenberg, A.; Blade, S.; Woods, S.; Bing, D.; Xue, A.; DeKoeyer, D.; et al. Quantitative trait loci for lodging resistance, plant height and partial resistance to mycosphaerella blight in field pea (*Pisum sativum* L.). *Theor. Appl. Genet.* **2003**, *107*, 1482–1491. [[CrossRef](#)]
19. Timmerman-Vaughan, G.M.; Frew, T.J.; Butler, R.; Murray, S.; Gilpin, M.; Falloon, K.; Johnston, P.; Lakeman, M.B.; Russell, A.; Khan, T. Validation of quantitative trait loci for Ascochyta blight resistance in pea (*Pisum sativum* L.), using populations from two crosses. *Theor. Appl. Genet.* **2004**, *109*, 1620–1631. [[CrossRef](#)]
20. Prioul, S.; Frankewitz, A.; Deniot, G.; Morin, G.; Baranger, A. Mapping of quantitative trait loci for partial resistance to *Mycosphaerella pinodes* in pea (*Pisum sativum* L.), at the seedling and adult plant stages. *Theor. Appl. Genet.* **2004**, *108*, 1322–1334. [[CrossRef](#)]
21. Fondevilla, S.; Satovic, Z.; Rubiales, D.; Moreno, M.T.; Torres, A.M. Mapping of quantitative trait loci for resistance to *Mycosphaerella pinodes* in *Pisum sativum* subsp. *syriacum*. *Mol. Breed.* **2008**, *21*, 439–454. [[CrossRef](#)]
22. Jha, A.B.; Tar'an, B.; Stonehouse, R.; Warkentin, T.D. Identification of QTLs associated with improved resistance to ascochyta blight in an interspecific pea recombinant inbred line population. *Crop Sci.* **2016**, *56*, 2926–2939. [[CrossRef](#)]
23. Jha, A.B.; Gali, K.K.; Tar'an, B.; Warkentin, T.D. Fine mapping of QTLs for Ascochyta blight resistance in pea using heterogeneous inbred families. *Front. Plant Sci.* **2017**, *8*, 765. [[CrossRef](#)]
24. Lee, R.C.; Grime, C.R.; O'Driscoll, K.; Khentry, Y.; Farfan-Caceres, L.M.; Tahghighi, H.; Kamphuis, L.G. Field pea (*Pisum sativum*) germplasm screening for seedling Ascochyta blight resistance and genome-wide association studies reveal loci associated with resistance to *Peyronellaea pinodes* and *Ascochyta koolunga*. *Phytopathology* **2023**, *113*, 265–276. [[CrossRef](#)]
25. Fondevilla, S.; Ávila, C.M.; Cubero, J.I.; Rubiales, D. Response to *Mycosphaerella pinodes* in a germplasm collection of *Pisum* spp. *Plant Breed.* **2005**, *124*, 313–315. [[CrossRef](#)]
26. Khan, T.W.; Keane, P.J.; Price, T.V. The epidemiology and control of Ascochyta blight in field peas: A review. *Aus. J. Agric. Res.* **2006**, *57*, 883–902. [[CrossRef](#)]
27. Boutet, G.; Lavaud, C.; Lesné, A.; Miteul, H.; Pilet-Nayel, M.L.; Andrivon, D.; Lejeune-Hénaut, I.; Baranger, A. Five regions of the pea genome co-control partial resistance to *D. pinodes*, tolerance to frost, and some architectural or phenological traits. *Genes* **2023**, *14*, 1399. [[CrossRef](#)] [[PubMed](#)]
28. Le May, C.; Ney, B.; Lemarchand, E.; Schoeny, A.; Tivoli, B. Effect of pea plant architecture on spatiotemporal epidemic development of ascochyta blight (*Mycosphaerella pinodes*) in the field. *Plant Pathol.* **2009**, *58*, 332–343. [[CrossRef](#)]
29. Richard, B.; Bussière, F.; Langrume, C.; Rouault, F.; Jumel, S.; Faivre, R.; Tivoli, B. Effect of pea canopy architecture on microclimate and consequences on ascochyta blight infection under field conditions. *Eur. J. Plant Pathol.* **2013**, *135*, 509–524. [[CrossRef](#)]
30. Banniza, S.; Hashemi, P.; Warkentin, T.D.; Vanderberg, A.; Davis, A.R. The relationships among lodging, stem anatomy, degree of lignification, and resistance to mycosphaerella blight in field pea (*Pisum sativum*). *Can. J. Bot.* **2005**, *83*, 954–967, Erratum in *Can. J. Bot.* **2005**, *83*, 1365. [[CrossRef](#)]
31. Tivoli, B.; Beasse, C.; Lemarchand, E.; Masson, E. Effect of ascochyta blight (*Mycosphaerella pinodes*) on yield components of single pea (*Pisum sativum*) plants under field conditions. *Ann. Appl. Biol.* **1996**, *129*, 207–216. [[CrossRef](#)]
32. Rubiales, D.; Fondevilla, S. Future prospects for ascochyta blight resistance breeding in cool season food legumes. *Front. Plant Sci.* **2012**, *3*, 27. [[CrossRef](#)]
33. Tran, H.S.; You, M.P.; Khan, T.N.; Barbetti, M.J. Relative host resistance to black spot disease in field pea (*Pisum sativum*) is determined by individual pathogens. *Plant Dis.* **2015**, *99*, 580–587. [[CrossRef](#)] [[PubMed](#)]
34. Joshi, S.; Pandey, B.R.; Rosewarne, G. Characterization of field pea (*Pisum sativum*) resistance against *Peyronellaea pinodes* and *Didymella pinodella* that cause ascochyta blight. *Front. Plant Sci.* **2022**, *13*, 976375. [[CrossRef](#)] [[PubMed](#)]
35. Rubiales, D.; Fernández-Aparicio, M.; Pérez-de-Luque, A.; Castillejo, M.A.; Prats, E.; Sillero, J.C.; Rispaill, N.; Fondevilla, S. Breeding approaches for crenate broomrape (*Orobanche crenata* Forsk.) management in pea (*Pisum sativum* L.) *Pest Manag. Sci.* **2009**, *65*, 553–559. [[CrossRef](#)]
36. Rubiales, D.; Osuna-Caballero, S.; González-Bernal, M.J.; Cobos, M.J.; Flores, F. Pea Breeding Lines Adapted to Autumn Sowings in Broomrape Prone Mediterranean Environments. *Agronomy* **2021**, *11*, 769. [[CrossRef](#)]
37. Zhang, R.; Hwang, S.-F.; Chang, K.-F.; Gossen, B.D.; Strelkov, S.E.; Turnbull, G.D.; Blade, S.F. Genetic resistance to *Mycosphaerella pinodes* in 558 field pea accessions. *Crop Sci.* **2006**, *46*, 2409–2414. [[CrossRef](#)]
38. Xue, A.G.; Warkentin, T.D. Partial resistance to *Mycosphaerella pinodes* in field pea. *Can. J. Plant Sci.* **2001**, *81*, 535–540. [[CrossRef](#)]

39. Česnulevičienė, R.; Gaurilėikienė, I.; Ramanauskienė, J. Control of ascochyta blight (*Ascochyta* complex) in pea under Lithuanian conditions. *Zemdirbyste-Agriculture* **2014**, *101*, 101–108. [[CrossRef](#)]
40. Pulse Breeding Australia. PBA Pearl: White Field Pea [Fact Sheet]. September 2012. Available online: <https://www.seednet.com.au/sites/seednet/files/2018-07/documents/PBA-Pearl-field-pea-factsheet.pdf> (accessed on 10 December 2025).
41. Tran, H.S.; You, M.P.; Khan, T.N.; Pritchard, I.; Barbetti, M.J. Resistance in field pea (*Pisum sativum*) to the black spot disease complex in Western Australia. *Eur. J. Plant Pathol.* **2014**, *140*, 597–605. [[CrossRef](#)]
42. Fondevilla, S.; Cubero, J.I.; Rubiales, D. Inheritance of resistance to *Mycosphaerella pinodes* in two wild accessions of *Pisum*. In *Ascochyta Blights of Grain Legumes*; Tivoli, B., Baranger, A., Muehlbauer, F.J., Cooke, B.M., Eds.; Springer: Dordrecht, The Netherlands, 2007; pp. 53–58. [[CrossRef](#)]
43. Fondevilla, S.; Küster, H.; Krajinski, F.; Cubero, J.I.; Rubiales, D. Identification of genes differentially expressed in a resistant reaction to *Mycosphaerella pinodes* in pea using microarray technology. *BMC Genom.* **2011**, *12*, 28. [[CrossRef](#)]
44. Instituto de Investigación y Formación Agraria y Pesquera (IFAPA), Junta de Andalucía. Red de Información Agroclimática de Andalucía (RIA). Available online: <https://www.juntadeandalucia.es/agriculturaypesca/ifapa/riaweb/web/> (accessed on 1 December 2025).
45. R Core Team. *R: A Language and Environment for Statistical Computing*, version 4.3.3; R Foundation for Statistical Computing: Vienna, Austria, 2024.
46. Bates, D.; Maechler, M.; Bolker, B.; Walker, S. *lme4: Linear Mixed-Effects Models using 'Eigen' and S4*, R package version 1.1.37; Comprehensive R Archive Network (CRAN): Vienna, Austria, 2025.
47. Kuznetsova, A.; Brockhoff, P.B.; Christensen, R.H.B. *lmerTest: Tests in Linear Mixed Effects Models*, R package version 3.1.3; Comprehensive R Archive Network (CRAN): Vienna, Austria, 2020.
48. Lenth, R.V.; Piaskowski, J. *EMMEANS: Estimated Marginal Means, aka Least-Squares Means*, R package version 1.11.2.8; Comprehensive R Archive Network (CRAN): Vienna, Austria, 2025.
49. Olivoto, T. *METAN: Multi Environment Trials Analysis*, R package version 1.19.0; Comprehensive R Archive Network (CRAN): Vienna, Austria, 2024.
50. Olivoto, T.; Nardino, M. MGIDI: Toward an effective multivariate selection in biological experiments. *Bioinformatics* **2021**, *37*, 3450–3456. [[CrossRef](#)]
51. Tivoli, B.; Baranger, A.; Avila, C.M.; Banniza, S.; Barbetti, M.; Chen, W.; Davidson, J.; Lindeck, K.; Kharrat, M.; Rubiales, D.; et al. Screening techniques and sources of resistance to foliar diseases caused by major necrotrophic fungi in grain legumes. *Euphytica* **2006**, *147*, 223–253. [[CrossRef](#)]
52. Roger, C.; Tivoli, B.; Huber, L. Effects of temperature and moisture on disease and fruit body development of *Mycosphaerella pinodes* on pea (*Pisum sativum*). *Plant Pathol.* **1999**, *48*, 1–9. [[CrossRef](#)]
53. Beeck, C.P.; Wroth, J.M.; Falk, D.E.; Khan, T.; Cowling, W.A. Two cycles of recurrent selection lead to simultaneous improvement in black spot resistance and stem strength in field pea. *Crop Sci.* **2008**, *48*, 2235–2244. [[CrossRef](#)]
54. Debnath, P.; Chakma, K.; Bhuiyan, M.S.U.; Thapa, R.; Pan, R.; Akhter, D. A novel multi trait genotype ideotype distance index (MGIDI) for genotype selection in plant breeding: Application, prospects, and limitations. *Crop Des.* **2024**, *3*, 1000074. [[CrossRef](#)]
55. Wang, T.F.; Gossen, B.D.; Slinkard, A.E. Lodging increases severity and impact of mycosphaerella blight on field pea. *Can. J. Plant Sci.* **2006**, *86*, 855–863. [[CrossRef](#)]
56. Schoeny, A.; Menat, J.; Darsonval, A.; Rouault, F.; Jumel, S.; Tivoli, B. Effect of pea canopy architecture on splash dispersal of *Mycosphaerella pinodes* conidia. *Plant Pathol.* **2008**, *57*, 1073–1085. [[CrossRef](#)]
57. Boros, L.; Marcinkowska, J. Assessment of selected pea genotypes reaction to *Ascochyta* blight under field conditions and the impact of disease severity on yield components. *J. Agric. Sci.* **2010**, *2*, 84–91. [[CrossRef](#)]
58. Daba, K.; Deokar, A.; Banniza, S.; Warkentin, T.D.; Tar'an, B. QTL mapping of early flowering and resistance to *ascochyta* blight in chickpea. *Genome* **2016**, *59*, 413–425. [[CrossRef](#)]
59. Conner, R.L.; Gossen, B.D.; Hwang, S.F.; Chang, K.F.; McRae, K.B.; Penner, W.C. Field assessment of partial resistance to mycosphaerella blight in *Pisum* subspecies accessions. *Can. J. Plant Sci.* **2012**, *92*, 289–296. [[CrossRef](#)]
60. Jha, A.B.; Warkentin, T.D.; Gurusamy, V.; Tar'an, B.; Banniza, S. Identification of *Mycosphaerella* blight resistance in wild *Pisum* species for use in pea breeding. *Crop Sci.* **2012**, *52*, 2462–2468. [[CrossRef](#)]
61. Annan, E.N.; Nyamesorto, B.; Yan, Q.; McPhee, K.; Huang, L. Optimized high throughput *Ascochyta* blight screening protocols and immunity to *Ascochyta pisi* in pea. *Pathogens* **2023**, *12*, 494. [[CrossRef](#)]
62. Jha, A.B.; Gali, K.K.; Banniza, S.; Warkentin, T.D. Validation of SNP markers associated with *ascochyta* blight resistance in pea. *Can. J. Plant Sci.* **2019**, *99*, 243–249. [[CrossRef](#)]
63. Castillejo, M.A.; Fondevilla, S.; Fuentes-Almagro, C. Quantitative analysis of target peptides related to resistance against *Ascochyta* blight (*Peyronella pinodes*) in pea. *J. Proteome Res.* **2020**, *19*, 1000–1012. [[CrossRef](#)]
64. Martins, L.B.; Balint-Kurti, P.; Reberg-Horton, S.C. Genome-wide association study for morphological traits and resistance to *Peyronella pinodes* in the USDA pea single plant plus collection. *G3 (Bethesda)* **2022**, *12*, jkac168. [[CrossRef](#)]

65. Carpenter, M.A.; Goulden, D.S.; Woods, C.J.; Thomson, S.J.; Kenel, F.; Frew, T.J.; Cooper, R.D.; Timmerman-Vaughan, G.M. Genomic selection for *Ascochyta* blight resistance in pea. *Front. Plant Sci.* **2018**, *9*, 1878. [[CrossRef](#)]
66. Jha, A.B.; Gali, K.K.; Alam, Z.; Lachagari, V.B.R.; Warkentin, T.D. Potential application of genomic technologies in breeding for fungal and oomycete disease resistance in pea. *Agronomy* **2021**, *11*, 1260. [[CrossRef](#)]

Disclaimer/Publisher's Note: The statements, opinions and data contained in all publications are solely those of the individual author(s) and contributor(s) and not of MDPI and/or the editor(s). MDPI and/or the editor(s) disclaim responsibility for any injury to people or property resulting from any ideas, methods, instructions or products referred to in the content.